JACS
JOURNAL OF THE AMERICAN CHEMICAL SOCIETY

Communication

pubs.acs.org/JACS

Direct Observation of Phenylalanine Orientations in Statherin Bound to Hydroxyapatite Surfaces

Tobias Weidner,*[,†,∥] Manish Dubey,[†,⊥] Nicholas F. Breen,[‡] Jason Ash,[‡] J. E. Baio,[†] Cherno Jaye,[§] Daniel A. Fischer,[§] Gary P. Drobny,[‡] and David G. Castner*[,†]

[†]National ESCA and Surface Analysis Center for Biomedical Problems, Departments of Bioengineering and Chemical Engineering, and [‡]Department of Chemistry, University of Washington, Seattle, Washington 98195, United States

[§]National Institute of Standards and Technology, Gaithersburg, Maryland 20899, United States

Supporting Information

ABSTRACT: Extracellular biomineralization proteins such as salivary statherin control the growth of hydroxyapatite (HAP), the principal component of teeth and bones. Despite the important role that statherin plays in the regulation of hard tissue formation in humans, the surface recognition mechanisms involved are poorly understood. The protein−surface interaction likely involves very specific contacts between the surface atoms and the key protein side chains. This study demonstrates for the first time the power of combining near-edge X-ray absorption fine structure (NEXAFS) spectroscopy with element labeling to quantify the orientation of individual side chains. In this work, the 15 amino acid N-terminal binding domain of statherin has been adsorbed onto HAP surfaces, and the orientations of phenylalanine rings F7 and F14 have been determined using NEXAFS analysis and fluorine labels at individual phenylalanine sites. The NEXAFS-derived phenylalanine tilt angles have been verified with sum frequency generation spectroscopy.

Proteins' interaction with and attachment to surfaces play a key role in biomaterials, tissue engineering, drug delivery, diagnostics, and biomimetics.[1−3] True molecular-level design in these fields requires high-resolution structure characterization to assess the conformation and orientation of adsorbed proteins along with specific structural motifs used by proteins to interact with surfaces. Traditional XRD and NMR structure analysis of protein crystals and solutions are extremely successful methods for obtaining high-resolution structures.[4,5] However, the conventional variants of XRD and NMR methods used for protein crystals or solutions do not have sufficient sensitivity for structure determination of monolayer or submonolayer concentrations of proteins bound on surfaces. Of the tens of thousands of protein structures reported, not a single structure of a protein on an inorganic surface has been solved.

Growing numbers of researchers are exploring possible routes to probe protein structure on surfaces using surface analytical tools such as sum frequency generation (SFG) spectroscopy,[6−20] IR and Raman spectroscopy,[21,22] time-of-flight secondary ion mass spectrometry (ToF-SIMS),[6,23−27] and near-edge X-ray absorption fine structure (NEXAFS) spectroscopy.[8,10,28−31] These techniques can provide information about the conformation, binding, and orientation of surface-bound proteins, but structural data for individual side chains within surface proteins, a crucial prerequisite for solving protein structures, have thus far only been obtained with SFG spectroscopy.[9] NEXAFS spectroscopy is of particular interest in this context owing to its inherent sensitivity to chemical bonds and molecular structure. It has been used to probe the global orientation and secondary structure of proteins, where libraries of amino acid and peptide spectra facilitate spectral assignments.[29−34] However, individual side chain structures within proteins have not yet been studied with this technique. Here we report a first observation of individual amino acid orientations in a surface-bound protein using NEXAFS spectra and side-chain element labeling. As a proof of concept, we obtain the phenyl ring orientations for individual phenylalanines (F) in the binding domain of the human biomineralization protein statherin adsorbed on a hydroxyapatite [HAP, $Ca_{10}(PO_4)_6(OH)_2$] surface. Mineralization proteins are excellent model systems for high-resolution surface analysis because typically they have high binding affinities and rigid surface structures.[3,35] These proteins act as nature's crystal engineers and adsorb onto crystal surfaces with precision using specific protein−surface binding motifs.[36]

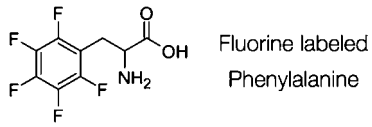

Figure 1. Labeling scheme used for the NEXAFS analysis.

The salivary statherin regulates HAP growth in bone and tooth enamel and prevents buildup of excess HAP by inhibiting spontaneous calcium phosphate growth.[37,38] Statherin also binds calcium ions in solution and inhibits precipitation of calcium ions out of supersaturated salivary solutions of calcium and phosphate ions.[39,40] In addition, statherin has a bacterial binding domain and can act as a lubricant.[41,42] The amino acid sequence of statherin is DSSEEKFLRRIGRFGYGYGPYQPV-PEQPLYPLQPYQPQYQQYTF.[43]

Statherin has been investigated in solution using solution NMR and CD spectroscopy, where it was found that statherin

Received: February 21, 2012
Published: May 7, 2012

   dx.doi.org/10.1021/ja301711w | J. Am. Chem. Soc. 2012, 134, 8750−8753

displays some transient helical structure in the N-terminal 15 amino acid peptide HAP binding domain, SN15.[44] Statherin bound to HAP crystals has been studied with binding isotherms and solid-state NMR (ssNMR). Drobny et al. published a series of ssNMR studies of the local secondary and tertiary structures of HAP-bound statherin as well as SN15,[45−48] where dipolar recoupling magic angle spinning techniques were used to study the surface proximity and dynamics of key acidic, basic, and nonpolar side chains.

The role of F in protein-HAP interactions is of particular interest because it has the largest HAP binding affinity of any amino acid with a nonpolar side chain.[49] Because two F residues are located within the HAP binding domain of statherin, we set out to explore the role of these side chains in HAP-protein recognition. It has been proposed, for example, that F may interact with HAP surfaces by exposing the delocalized electrons of the phenyl ring.[49] Phenylalanines do not nucleate ions because they are nonpolar, but they may play a role in the recognition of HAP surfaces.

SN15 $^{13}C\{^{31}P\}$ REDOR NMR experiments showed residues F7 and F14 oriented quite differently relative to the HAP surface: a small REDOR response indicated the phenyl ring of F7 was at least 7 Å from the HAP surface, while the phenyl ring of F14 elicited a much stronger $^{13}C\{^{31}P\}$ REDOR signal, indicating it was within 4 Å of the HAP surface.[46]

Here we use NEXAFS spectroscopy to study the orientations of these F7 and F14 side chains. NEXAFS has proven to be a powerful tool to probe protein structure and binding on surfaces,[27] is extremely sensitive to surface chemical bonds, and can provide detailed information about the chemistry and orientation of surface species. One difficulty of protein structure analysis using NEXAFS is the wide variety and abundance of chemical bonds in all proteins and most peptides. While backbone amide bonds with different orientations throughout a protein can sometimes be averaged to an apparent amide vector and thus provide some general understanding of the orientation of entire proteins,[6,8,28] this approach obviously cannot be applied to understanding details in the side-chain structure. To address this problem, we synthesized two SN15 peptides with hydrogens in the F rings substituted by fluorine in either F7 (SN15-F7) or F14 (SN15-F14). The unique C−F bonds acted as residue-specific element labels and could be individually interrogated with NEXAFS spectroscopy (Figure 1).

The SN15-F7 and SN15-F14 peptides were adsorbed onto artificial HAP surfaces, prepared by mineral precipitation from a supersaturated simulated body fluid.[50] HAP growth and peptide monolayer formation was verified using X-ray photoelectron spectroscopy and ToF-SIMS (see Supporting Information).

Figure 2 shows fluorine K-edge NEXAFS spectra collected using X-ray incidence angles of 70, 55, and 20° for SN15-F7 and SN15-F14 monolayer films on HAP. The low surface density of the fluorinated rings leads to a comparatively low signal/noise ratio. Assuming a width of ∼15 Å and a length of ∼28 Å, we estimate the surface area per peptide, and thus per fluorophenyl ring, to be ∼420 Å^2. The fluorophenyl surface density is ∼15−19 times lower than that of typical aromatic self-assembled monolayers with a 22−27 Å^2 footprint per molecule.[51] We compensated for the low signal/noise ratio by averaging over 5−10 spectra collected at different positions on the samples for each angle. The spectra exhibit characteristic absorption resonances of the fluorophenyl rings. The peak near 690.9 eV is most prominent for both peptides and can clearly be assigned to the fluorine 1s→π_1*(C−C) transition.[52,53] A

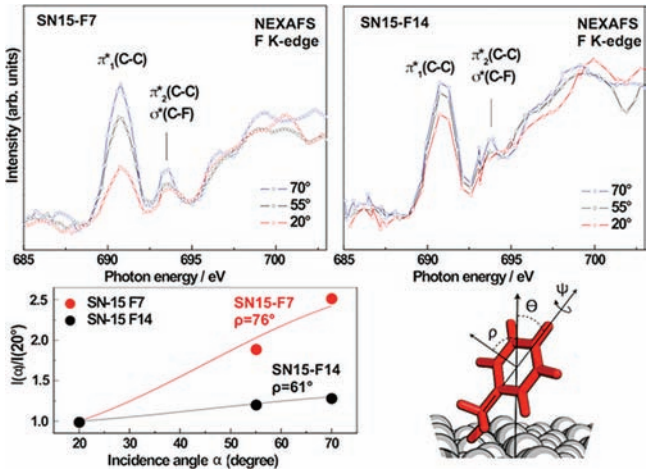

Figure 2. (Top) F K-edge NEXAFS spectra of SN15-F7 and -F14 adsorbed onto on HAP surfaces acquired at X-ray incidence angles α = 70, 55, and 20°. (Bottom) Angular dependence of π_1* resonance intensity ratio $I(\alpha)/I(20°)$ for SN15-F7 and -F14. The diagram shows the angles used in characterizing SN15, including the tilt angles ρ of the phenyl ring plane normal with respect to the surface normal.

weaker peak near 693.8 eV is assigned to the corresponding π_2* resonance, overlapping with contributions from a fluorine 1s→σ*(C−F) excitation. Since the intense π_1* resonance is representative of the π*-orbital which is delocalized over the entire fluorophenyl molecule, we can use the angular dependence of the resonance intensity to determine the orientation of the rings using well-established procedures for analogous hydrogenated phenyl moieties.[54,55] Spectra from both SN15-F7 and SN15-F14 exhibit considerable linear dichroism—a dependence of the absorption resonance intensity on the X-ray incidence angle. A significant dichroism is considered a fingerprint of orientational order. The intensity of photo excitation resonances depends on the relative orientations of the electric field vector of the X-rays with respect to the target molecular orbital. The transition dipole moment (TDM) of π* resonances is oriented perpendicular to the phenyl ring plane. A higher intensity at an X-ray incident angle of 70° compared to 20° suggests that the fluorophenyl moieties in SN15-F7 and SN15-F14 have a predominately upright orientation with respect to the surface. The difference in the angular dependence between SN15-F7 and SN15-F14 (larger for SN15-F7) implies a more tilted orientation for F14 with respect to the surface normal: the F14 ring plane is closer to parallel to the surface. The lower dichroic ratio for F14 could also result from a lower degree of order or a higher mobility. However, since ssNMR results for SN15 on HAP particles show that F14 is closer to the surfaces than F7,[46] F14 is expected to have a stronger interaction with the surface and thus a more ordered configuration than F7. This view is supported by the SFG data discussed below. An additional, detailed ssNMR study of F dynamics in HAP-bound SN15 is underway and will be published in the future.

The ring orientation was evaluated by monitoring the intensity of the π_1* absorption resonances as a function of the X-ray incidence angle. The resulting intensity dependence was analyzed according to an established textbook procedure for aromatic rings.[54] The π_1* intensities for different incidence angles are plotted and then fit to the following expression:[54]

dx.doi.org/10.1021/ja301711w | J. Am. Chem. Soc. 2012, 134, 8750−8753

$$I(\alpha,\rho) = A\left(P\frac{1}{3}\left[1 + \frac{1}{2}(3\cos^2\rho - 1)(3\cos^2\rho - 1)\right] + (1-P)\frac{1}{2}\sin^2\alpha\right)$$

where A is a constant, P is the polarization factor of the synchrotron light, α is the X-ray incidence angle, and ρ is the average tilt angle of the TDM associated to the molecular orbital (all angles are defined with respect to the surface normal). Intensity normalization problems were minimized by considering intensity ratios, $I(\alpha)/I(20°)$, instead of the absolute values (see Figure 2 for details of the involved angles). The dependence on α is displayed in Figure 2, along with the respective fits according to this equation. The phenyl ring plane is normal to the orientation of the π_1* orbitals. The derived tilt angles ρ for the normal of the fluorophenyl ring planes are 76° for F7 and 61° ± 7° for F14.

A model was developed for SN15 adsorbed onto HAP indicating F7 and F14 ring orientations that are consistent with the NEXAFS data and published constraints based on ssNMR data. The NEXAFS-determined tilt angles were tested with independent measurements of the phenyl ring orientations using SFG spectroscopy. We have shown previously that SFG can probe the orientations of individual side chains on surfaces if combined with isotope labels.[9] Here we take advantage of the fact that the fluorine-labeled SN15 peptides have only one hydrogenated aromatic side chain. Details of the experimental setup and the data analysis can be found in the Supporting Information. Since the aromatic C−H resonances are well separated from the background of aliphatic modes below 3000 cm^{-1}, the F rings can be probed individually with SFG. Figure 3

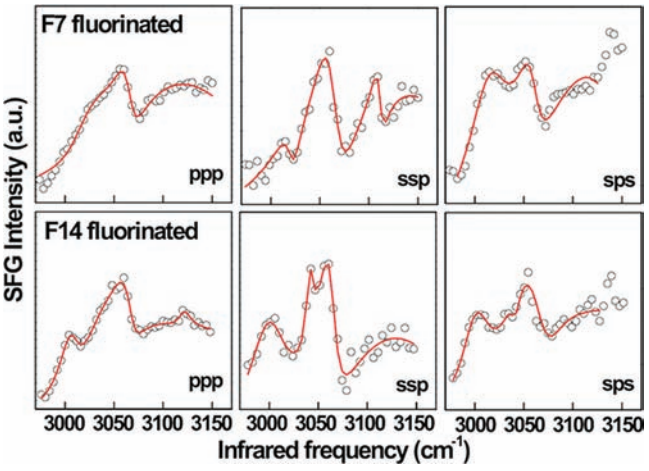

Figure 3. SFG spectra for SN15-F7 and -F14 recorded in situ in PBS buffer using different polarization combinations. The spectra of SN15-F7 are representative of ring F14, and the spectra of SN15-F14 are representative of ring F7.

shows SFG spectra recorded using ssp (s-polarized SFG, s-polarized visible, and p-polarized IR), ppp, and sps polarization combinations for SN15-F14 and SN15-F7. The main spectral features are resonances near 3022 and 3060 cm^{-1}, related to the ν_{20A} and ν_2 modes of the phenyl rings, respectively.[56,57] The ring tilt and twist angles (Θ and ψ, see Figure 2) were determined using ν_2 peak intensity ratios determined from the ssp, ppp, and sps spectra following published procedures for polystyrene phenyl rings.[56] This analysis yielded Θ = 11° and ψ = 15° for F7 and Θ = 34° and ψ = 35° for F14. The general accuracy of these values is ±6°, which reflects experimental factors and the analysis procedure. The orientation of the ring plane normal ρ is related to the tilt and twist angles according to $\rho = \arccos(\sin\Theta\cos\psi)$.The resulting SFG-determined ring orientations ρ are 80° for F7 and 63° for F14. These values compare well with the NEXAFS-determined angles (76° for F7 and 61° for F14).

For additional insight into the F side-chain structure, the NEXAFS- and SFG-determined ring orientations and positions can be combined with published structural data obtained from ssNMR. Using distance measurements and side chain dynamics, Gibson at al. determined that F14 is close to the HAP (∼4 Å) with its 2′-4′ and 5′-6′ axes at equal distances to the surface.[46] F7 was found to be farther from the surface (>6.5 Å). NEXAFS is sensitive to ring orientation but cannot directly distinguish between different directions. Comparing NMR and NEXAFS results (distance, ring rotation), we conclude that the phenyl ring of F14 points toward the surface with a C1−C4 axis angle of 33°. F7 was found to be more dynamic than F14 according to ssNMR and most likely undergoes two-site jumps between different orientations with high frequency. The NEXAFS- and SFG-based orientation is thus a time average of the two conformers, and a study combining ssNMR line shape simulations and NEXAFS analysis is underway to address this complex question in more detail. Based on NMR data, we can conclude that on average F7 points away from the surface with a ring orientation of 11°. Based on this information and steric constraints from published ssNMR data about the orientation of neighboring side chains,[42,58,59] we can estimate the F7 and F14 side-chain orientations. Figure 4 displays a possible

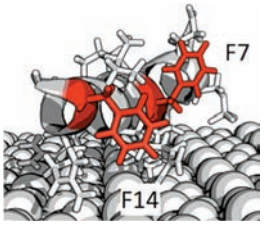

Figure 4. Model of SN-15 adsorbed onto HAP indicating F7 and F14 ring orientations that are consistent with the NEXAFS and SFG data as well as published constraints based on ssNMR data.

structure for SN15 on HAP that takes into account the NEXAFS and SFG angles and surface distance data as well as structural parameters from previous ssNMR studies. Admittedly, this model is only one of a number of possible structures. However, this study has shown that NEXAFS spectroscopy can provide detailed information about side-chain structure if combined with element labels. A promising approach to further refine our picture of SN15 on HAP will be to combine our findings with additional experimental data (e.g., from SFG amide I measurements) and use the determined structural parameters to guide and constrain computational methods, such as MD simulations.[58,60]

■ ASSOCIATED CONTENT

Ⓢ Supporting Information

Experimental and analysis details. This material is available free of charge via the Internet at http://pubs.acs.org.

■ AUTHOR INFORMATION

Corresponding Author

weidner@mpip-mainz.mpg.de; castner@uw.edu

Present Addresses

[‖]Max Planck Institute for Polymer Research, Germany
[⊥]Intel Corp., Chandler, AZ

Notes

The authors declare no competing financial interest.

■ ACKNOWLEDGMENTS

This work was funded in part by NIH grants DE-012554 and EB-002027 (NESAC/BIO). T.W. thanks the German Research Foundation for a research fellowship (We 4478/1-1). NEXAFS studies were performed at the NSLS, Brookhaven National Laboratory, which is supported by the U.S. Department of Energy, Division of Materials Science and Division of Chemical Sciences.

■ REFERENCES

(1) Horbett, T. A.; Brash, J. L. *Proteins at Interfaces II: Fundamentals and Applications*; American Chemical Society: Washington, DC, 1995.
(2) Castner, D. G.; Ratner, B. D. *Surf. Sci.* **2002**, *500*, 28.
(3) Hildebrand, M. *Chem. Rev.* **2008**, *108*, 4855.
(4) Cavanagh, J.; Fairbrother, W. J.; Palmer, A. G., III; Rance, M.; Skelton, N. J. *Protein NMR spectroscopy: principles and practice*, 2nd ed.; Academic Press: Boston, MA, 2007.
(5) Rupp, B. *Biomolecular Crystallography: Principles, Practice and Application to Structural Biology*; Garland Science: New York, 2009.
(6) Baugh, L.; Weidner, T.; Baio, J. E.; Nguyen, P. C. T.; Gamble, L. J.; Slayton, P. S.; Castner, D. G. *Langmuir* **2010**, *26*, 16434.
(7) Breen, N. F.; Weidner, T.; Li, K.; Castner, D. G.; Drobny, G. P. *J. Am. Chem. Soc.* **2009**, *131*, 14148.
(8) Weidner, T.; Apte, J. S.; Gamble, L. J.; Castner, D. G. *Langmuir* **2010**, *26*, 3433.
(9) Weidner, T.; Breen, N. F.; Li, K.; Drobny, G. P.; Castner, D. G. *P. Natl. Acad. Sci. U.S.A.* **2010**, *107*, 13288.
(10) Weidner, T.; Samuel, N. T.; McCrea, K.; Gamble, L. J.; Ward, R. S.; Castner, D. G. *Biointerphases* **2010**, *5*, 9.
(11) Chen, Z.; Ward, R.; Tian, Y.; Malizia, F.; Gracias, D. H.; Shen, Y. R.; Somorjai, G. A. *J. Biomed. Mater. Res.* **2002**, *62*, 254.
(12) Mermut, O.; Phillips, D. C.; York, R. L.; McCrea, K. R.; Ward, R. S.; Somorjai, G. A. *J. Am. Chem. Soc.* **2006**, *128*, 3598.
(13) Phillips, D. C.; York, R. L.; Mermut, O.; McCrea, K. R.; Ward, R. S.; Somorjai, G. A. *J. Phys. Chem. B* **2007**, *111*, 255.
(14) York, R. L.; K., B. W.; Geissler, P. L.; Somorjai, G. A. *Isr. J. Chem.* **2007**, *47*, 51.
(15) York, R. L.; Mermut, O.; Phillips, D. C.; McCrea, K. R.; Ward, R. S.; Somorjai, G. A. *J. Phys. Chem. B* **2007**, *111*, 8866.
(16) Wang, J.; Buck, S. M.; Chen, Z. *J. Phys. Chem. B* **2002**, *106*, 11666.
(17) Wang, J.; Chen, X. Y.; Clarke, M. L.; Chen, Z. *Proc. Natl. Acad. Sci. U.S.A.* **2005**, *102*, 4978.
(18) Yang, P.; Ramamoorthy, A.; Chen, Z. *Langmuir* **2011**, *27*, 7760.
(19) Ye, S.; Nguyen, K. T.; Le Clair, S. V.; Z., C. *J. Struct. Biol.* **2009**, *168*, 61.
(20) Fu, L.; Liu, J.; Yan, E. C. Y. *J. Am. Chem. Soc.* **2011**, *133*, 8094.
(21) Ataka, K.; Heberle, J. *Anal. Bioanal. Chem.* **2007**, *388*, 47.
(22) Pettinger, B. *Mol. Phys.* **2010**, *108*, 2039.
(23) Baio, J. E.; Weidner, T.; Interlandi, G.; Mendoza-Barreraa, C.; Canavan, H. E.; Michel, R.; Castner, D. G. *J. Vac. Sci. Technol., B* **2011**, *29*, 04D113.
(24) Lhoest, J. B.; Detrait, E.; van den Bosch de Aguilar, P.; Bertrand, P. *J. Biomed. Mater. Res. A* **1998**, *41*, 95.
(25) Xia, N.; May, C. J.; McArthur, S. L.; Castner, D. G. *Langmuir* **2002**, *18*, 4090.
(26) Wang, H.; Castner, D. G.; Ratner, B. D.; Jiang, S. Y. *Langmuir* **2004**, *20*, 1877.
(27) Baio, J. E.; Weidner, T.; Samuel, N. T.; McCrea, K.; Baugh, L.; Stayton, P. S.; Castner, D. G. *J. Vac. Sci. Technol., B* **2010**, *28*, C5D1.
(28) Liu, X.; Jang, C.-H.; Zheng, F.; Jürgensen, A.; Denlinger, J. D.; Dickson, K. A.; Raines, R. T.; Abbott, N. L.; Himpsel, F. J. *Langmuir* **2006**, *22*, 7719.
(29) Zubavichus, Y.; Shaporenko, A.; Grunze, M.; Zharnikov, M. *J. Phys. Chem. B* **2007**, *111*, 11866.
(30) Zubavichus, Y.; Zharnikov, M.; Schaporenko, A.; Grunze, M. *J. Electron Spectrosc. Relat. Phenom.* **2004**, *134*, 25.
(31) Gordon, M. L.; Cooper, G.; Morin, C.; Araki, T.; Turci, C. C.; Kaznatcheev, K.; Hitchcock, A. P. *J. Phys. Chem. A* **2003**, *107*, 6144.
(32) Zubavichus, Y.; Shaporenko, A.; Grunze, M.; Zharnikov, M. *J. Phys. Chem. A* **2005**, *109*, 6998.
(33) Zubavichus, Y.; Shaporenko, A.; Grunze, M.; Zharnikov, M. *J. Phys. Chem. B* **2006**, *110*, 3420.
(34) Cooper, G.; Gordon, M.; Tulumello, D.; Turci, C.; Kaznatcheev, K.; Hitchcock, A. P. *J. Electron Spectrosc. Relat. Phenom.* **2004**, *137*, 795.
(35) Mann, S. *Nature* **1988**, *332*, 119.
(36) *Handbook of Biomineralization: Biomimetic and Bioinspired Chemistry*; Behrens, P, Bäuerlein, E., Eds.; Wiley-VCH: Weinheim, Germany, 2009; Vol. *2*.
(37) Proctor, G. B.; Hamdan, S.; Carpenter, G. H.; Wilde, P. *Biochem. J.* **2005**, *389*, 111.
(38) Hay, D. I.; Moreno, E. C. *Human Saliva: Clinical Chemistry and Microbiology*; CRC: Boca Raton, FL, 1989; Vol. *1*.
(39) Moreno, E.; Varughese, K.; Hay, D. *Calcif. Tissue Int.* **1979**, *28*, 7.
(40) Goobes, R.; Goobes, G.; Shaw, W. J.; Drobny, G. P.; Campbell, C. T.; Stayton, P. S. *Biochemistry* **2007**, *46*, 4725.
(41) Sekine, S.; Kataoka, K.; Tanaka, M.; Nagata, H.; Kawakami, T.; Akaji, K.; Aimoto, S.; Shizukuishi, S. *Microbiology* **2004**, *150*, 2373.
(42) Goobes, G.; Goobes, R.; Schueler-Furman, O.; Baker, D.; Drobny, G. P. *Proc. Natl. Acad. Sci. U.S.A.* **2006**, *103*, 16083.
(43) Ulrich, E. L.; Akutsu, H.; Doreleijers, J. F.; Harano, Y.; Ioannidis, Y. E.; Lin, J.; Livny, M.; Mading, S.; Maziuk, D.; Miller, Z.; Nakatani, E.; Schulte, C. F.; Tolmie, D. E.; Kent Wenger, R.; Yao, H.; Markley, J. L. *Nucleic Acids Res.* **2008**, *36*, D402.
(44) Naganagowda, G. A.; Gururaja, T. L.; M.J., L. *J. Biomol. Struct. Dyn.* **1998**, *16*, 91.
(45) Ndao, M.; Ash, J. T.; Breen, N. F.; Goobes, G.; Stayton, P. S.; Drobny, G. P. *Langmuir* **2009**, *25*, 12136.
(46) Gibson, J. M.; Popham, J. M.; Raghunathan, V.; Stayton, P. S.; Drobny, G. P. *J. Am. Chem. Soc.* **2006**, *128*, 5364.
(47) Gibson, J. M.; Raghunathan, V.; Popham, J. M.; Stayton, P. S.; Drobny, G. P. *J. Am. Chem. Soc.* **2006**, *127*, 9350.
(48) Shaw, W. J.; Long, J. R.; Dindot, J. L.; Campbell, A. A.; Stayton, P. S.; Drobny, G. P. *J. Am. Chem. Soc.* **2000**, *122*, 1709.
(49) Koutsopoulos, S.; Dalas, E. *Langmuir* **2000**, *16*, 6739.
(50) Toworfe, G. K.; Composto, R. J.; Shapiro, I. M.; Ducheyne, P. *Biomaterials* **2006**, *27*, 631.
(51) Cyganik, P.; Buck, M. *J. Am. Chem. Soc.* **2004**, *126*, 5960.
(52) Hitchcock, A. P.; Fischer, P.; Gedanken, A.; Robin, M. B. *J. Phys. Chem.* **1987**, *91*, 531.
(53) Plashkevych, O.; Yang, L.; Vahtras, O.; Ågren, H.; Pettersson, L. G. M. *Chem. Phys.* **1997**, *222*, 125.
(54) Stöhr, J. *NEXAFS Spectroscopy*; Springer-Verlag: Berlin, Germany, 1992; Vol. *25*.
(55) Chesneau, F.; Schupbach, B.; Szelagowska-Kunstman, K.; Ballav, N.; Cyganik, P.; Terfort, A.; Zharnikov, M. *Phys. Chem. Chem. Phys.* **2010**, *12*, 12123.
(56) Briggman, K. A.; Stephenson, J. C.; Wallace, W. E.; Richter, L. J. *J. Phys. Chem. B* **2001**, *105*, 2785.
(57) Varsanyi, G. *Assignments for Vibrational Spectra of Seven Hundred Benzene Derivatives*; Adam Hilger: London, 1974; Vol. *1.1*, *1.2*, *2*.
(58) Masica, D. L.; Ash, J. T.; Ndao, M.; Drobny, G. P.; Gray, J. J. *Structure* **2010**, *18*, 1678.
(59) Ndao, M.; Ash, J. T.; Stayton, P. S.; Drobny, G. P. *Surf. Sci.* **2010**, *604*, L39.
(60) Makrodimitris, K.; Masica, D. L.; Kim, E. T.; Gray, J. J. *J. Am. Chem. Soc.* **2007**, *129*, 13713.